Pumping new life into preclinical pharmacokinetics: exploring the pharmacokinetic application of ex vivo organ perfusion

Stevens, L.J.

PART II

The liver perfusion model to study drug pharmacokinetic processes and endogenous substrate handling

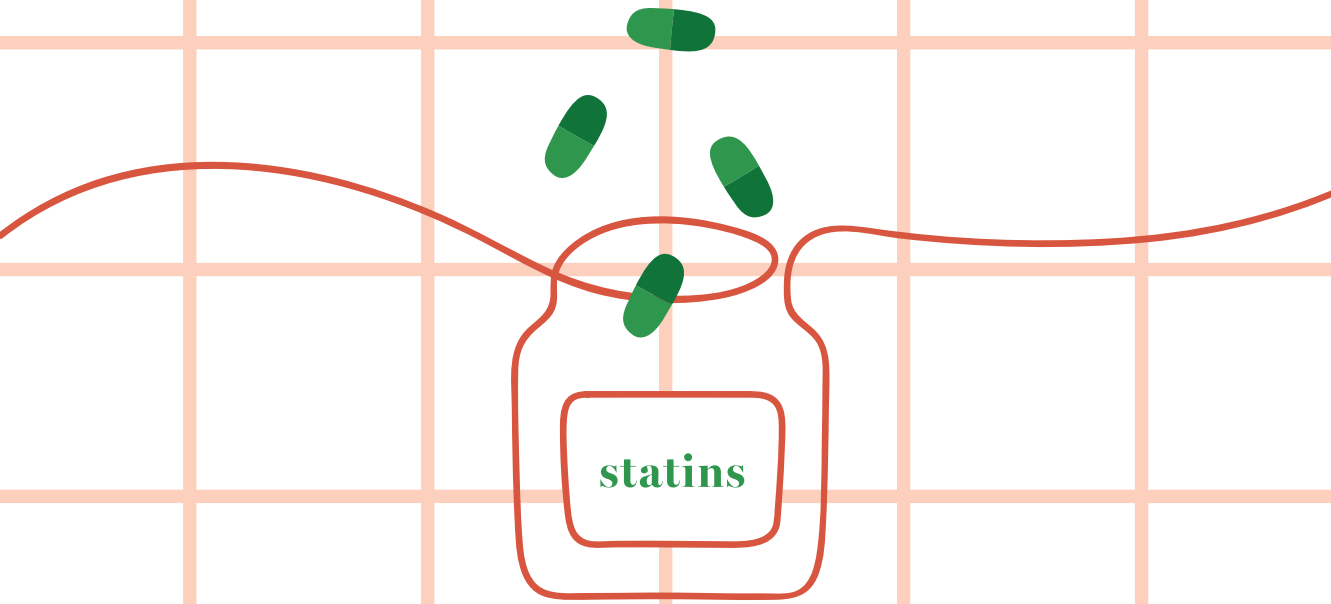
statins

CHAPTER 03

Evaluation of normothermic machine perfusion of porcine livers as a novel preclinical model to predict biliary clearance and transporter-mediated drug-drug interactions using statins

L.J. Stevens, A.Z.X. Zhu, P.P. Chothe, S.K. Chowdhury, J.M. Donkers, W.H.J. Vaes, C.A.J. Knibbe, I.P.J. Alwayn, E. van de Steeg

Drug Metabolism and Disposition, 2021

Abstract

There is a lack of translational preclinical models that can predict hepatic handling of drugs. In this study we aimed to evaluate the applicability of normothermic machine perfusion (NMP) of porcine livers as a novel *ex vivo* model to predict hepatic clearance, biliary excretion and plasma exposure of drugs. For this evaluation we dosed atorvastatin, pitavastatin and rosuvastatin as model drugs to porcine livers and studied the effect of common drug-drug interactions (DDI) on these processes. After 120 min of perfusion, 0.104 mg atorvastatin (n=3), 0.140 mg pitavastatin (n=5) or 1.4 mg rosuvastatin (n=4) was administered to the portal vein, 120 min later followed by a second bolus of the statin co-administrated with OATP perpetrator drug rifampicin (67.7 mg). Following the first dose, all statins were rapidly cleared from the circulation (hepatic extraction ratio > 0.7) and excreted into the bile. Presence of human specific atorvastatin metabolites confirmed the metabolic capacity of porcine livers. The predicted biliary clearance of rosuvastatin was found to be closer to the observed biliary clearance. A rank-order of the DDI between the various systems upon co-administration with rifampicin could be observed: atorvastatin (AUC Ratio 7.2)> rosuvastatin (AUC Ratio 3.1)> pitavastatin (AUC Ratio 2.6) which is in good agreement with the clinical DDI data. The results from this study demonstrated the applicability of using NMP of porcine livers as a novel preclinical model to study OATP-mediated DDI and its effect on hepatic clearance, biliary excretion and plasma profile of drugs.

Introduction

The liver is a complex organ involved in the uptake, metabolism and biliary excretion of xenobiotics and endogenous compounds. Transporters located at the basolateral side of the plasma membrane, like the Organic Anion-Transporting Peptides (OATP) 1B1, 1B3, 2B1, Na^+-taurocholate cotransporting polypeptide (NTCP) and the Organic Anion Transporter (OAT) 2, are involved in the uptake of drugs and endogenous compounds from the portal and arterial circulation into hepatocytes[1-3]. After uptake, compounds can be metabolized, for example by the cytochrome P450 (CYP450) family of enzymes, and subsequently effluxed into the bile across the canalicular membrane or back into the systemic circulation across the sinusoidal membrane[4]. Several transporters are involved in the hepatic efflux, including multidrug resistance protein 1 (MDR1; P-glycoprotein), breast cancer resistance protein (BCRP), bile salt export pump (BSEP) and multidrug resistance-associated protein 2 (MRP2) at the canalicular membrane and multidrug resistance-associated protein 3 and 4 (MRP3 and MR4) at the basolateral membrane. Concomitant administration of drugs that are substrates for the same transporters and/or metabolizing enzymes can result in a drug-drug interaction (DDI) affecting plasma as well as biliary levels of one of the drugs . As a result, this can change the drug concentration at the target, or it can even lead to toxicity (e.g. drug induced liver injury (DILI)). Therefore, interactions affecting hepatic uptake and biliary excretion are important to characterize in the preclinical phase of drug development[5,6].

To evaluate the potential DDI for newly developed drugs, the FDA stated that it is important to understand the principal route of the drug's elimination and to understand the contribution and effect of the drug on transporters and metabolizing enzymes. Especially DDI at the transporter level is important to characterize since they control the absorption, distribution and elimination of the drug in various organs[7]. When a newly developed drug for example is intended to be used by a population which is likely to also use statins, the sponsor should examine the potential of the investigational drug to interact with OATP1B1/1B3[7].

To study complex processes such as transporter-enzyme interplay, potential DDI and biliary excretion, physiologically relevant models are needed which recapitulate all functions of the liver including the ability to produce bile[8]. The

sandwich cultured hepatocyte and rat liver perfusion models are known to capture these complex processes and are currently used to investigate hepatobiliary disposition of drugs. Unfortunately, these models have their own limitations. *In vitro* to *in vivo* translation often fails due to species differences or due to differences in transporter expression resulting in difficulties in the prediction of plasma profiles after oral and intravenous administration[9]. Therefore, extrapolation of data obtained using rodent models is not feasible for the prediction of human PK and DDI[9-11].

At present, research in the field of organ transplantation is focused on organ preservation techniques using machine perfusion. These pressure driven perfusion machines are able to perfuse human and porcine livers at a physiological pressure under oxygenated and normothermic conditions. Porcine organs are often used for method validation and device development and it has been shown that normothermic machine perfusion (NMP) of the porcine liver is an excellent platform to study hepatic processes[12,13]. The pig model is considered as a proper translational model because of anatomical, physiological and biochemical similarity to humans and nowadays this model is increasingly used in biomedical research[14]. Compared to the rat model, the size of the pig model supports the collection of larger sample volumes and there is the ability to take tissue biopsies in time. Furthermore, an advantage of using livers from pig origin is the similarity of Phase I and Phase II biotransformation reactions[14], which was recently confirmed in a quantitative proteomic analysis comparing transporter and metabolizing enzyme expression in human and porcine liver[15].

In this study, we evaluate using normothermic machine perfusion of porcine livers as a novel preclinical model to predict pharmacokinetic processes. Using three statins as model drug compounds (rosuvastatin, atorvastatin and pitavastatin) we studied the transporter mediated hepatic extraction and biliary excretion. Additionally, we examined the effect of rifampicin on the disposition of these three statins.

Materials and method

Chemicals

Atorvastatin, Pitavastatin and rifampicin were purchased from Bio-Connect (Huissen, the Netherlands). Rosuvastatin calcium, Heparin, taurocholate and insulin were purchased Sigma-Aldrich Chemie B.V. (Zwijndrecht, the Netherlands). Atorvastatin lactone, 2-hydroxy atorvastatin, 2-hydroxy atorvastatin lactone, 4-hydroxy atorvastatin and 4-hydroxy atorvastatin lactone were obtained from Toronto Research Chemicals (Toronto, ON, Canada). Epoprostenol was purchased from R&D systems (Minneapolis, USA). Vitamin solution, L-glutamine, MEM essential acids and glutamax were obtained from Gibco (Paisley, Scotland). Calcium gluconate 10% was obtained from Pharmamarket (Hove, Belgium).

Porcine livers

Livers were obtained from a local slaughterhouse (*Sus scrofa domesticus*, approximately at age of 6 months with body weight between 100 and 120 kg). Pigs were sacrificed by a standardized procedure of electrocution followed by exsanguination. Thereafter, three liters of blood was collected in a container supplemented with 25000 IU of heparin. All abdominal organs were dissected outside the animal and collected. Within 20 min after termination, the *vena porta* was cannulated and directly flushed by gravity with 3L of NaCl 0.9% (Baxter BV, Utrecht the Netherlands) supplemented with 5000 IU of heparin followed by 2L of ice-cold Histidine-Tryptophan-Ketoglutarate (HTK) solution (Plegistore, Warszawa in Poland). In the meantime, the *arteria hepatica* was dissected, cannulated and subsequently flushed with HTK. At the laboratory, side branches were ligated, the common bile duct was cannulated while the *ductus cysticus,* derived from the gall bladder, was ligated.

Normothermic machine perfusion

The porcine livers were perfused using the LiverAssist device (Organ Assist, Groningen, the Netherlands). The machine consists of two rotary pumps that provide a pulsatile flow to the hepatic artery and a continuous flow to the portal vein. The system was filled with 2L perfusion fluid containing red blood cells and plasma (Supplemental Table S3.1). Insulin, taurocholate, heparin and epoprostenol were provided as continuous infusion at a rate of 10U/h, 1041U/h, 10 mL/h (2% w/v) and 8 µg/h, respectively, in order to maintain liver

functioning including bile flow. Additionally, amino acids and vitamins were continuous provided to keep the liver metabolically active (Supplementarl Table S3.1). Gas delivery to the LiverAssist consisted of 95% oxygen and 5% carbon dioxide at 2L/min and the temperature was set at 39°C (body temperature pigs). The livers were perfused with a portal pressure of 11 mmHg and a mean arterial pressure of 50 mmHg. Upon perfusion, additional boluses of sodium bicarbonate and glucose were applied depending on perfusate pH (range 7.35–7.45) and glucose concentration (>5 mmol/L). Arterial blood gas samples were taken hourly to monitor liver viability (pH, glucose, Na, K, lactate etc.) using the i-STAT clinical analyzer (Abbot Point of Care Inc., Princeton, NJ).

Drug administration during perfusion

The plasma and biliary concentration of atorvastatin, rosuvastatin and pitavastatin and rifampicin were determined. Additionally, atorvastatin metabolite formation was determined. The statins and rifampicin were selected based on clinically known DDI and *in vitro* transporter study data and are presented in Table 3.1. Initial portal doses for atorvastatin and rifampicin applied to the system were based on simulations by SimCyp. After pilot experiments, the doses were increased 2x for atorvastatin (0.052 mg to 0.104 mg) and 3x for rifampicin (22.6 mg to 67.7 mg) to facilitate proper detection by LCMS. For the other two statins, rosuvastatin and pitavastatin, the compound profiles were not available in SimCyp. Therefore the portal doses of rosuvastatin and pitavastatin were based on the oral dosage and corrected for the fraction absorbed (F_a), average correction for Fraction escaping the gut (Fg) (0.7) (16) and corrected for the total circulating volume of 2L in the perfusion system (compared to 5L *in vivo*). To study DDI, the set-up as depicted in Figure 1 was applied. After a stabilization period of 120 min, the statin was administered at as a slow bolus at a rate of 1mL/min during 10 min to the portal vein. Time of starting the slow bolus was set at t=0 min. Subsequently, plasma and bile samples were taken for the following 120 min. Arterial blood samples were taken at t=0, 2, 4, 6, 8, 10, 15, 20, 30, 40, 50, 60, 90 and 120 min. Portal samples were taken during the administration of the drug at t=5 and t=10 min to determine the first pass effect. This portal sampling point was ~30cm from the portal dosing point. Bile samples were collected in 10-minute fractions. Blood samples were centrifuged directly after collection at 1.3 *g* for 10 min at 4°C and thereafter plasma (and bile) samples were immediately stored at ≤-70°C until further processed. Drug concentrations in plasma, bile and liver biopsies were determined by LC-MS/MS analysis as described below.

At 120 min, biopsies were taken (n=2) to determine the intracellular concentration in the hepatocytes. After the first 120 min, a slow bolus 10 min (1mL/min) of 67.7 mg rifampicin was administered to the liver and after 5 min (t=125 min), a subsequent slow bolus of the statin was administrated to the portal vein of the liver. The same sampling schedule for the following 120 min was applied. After the last sampling time point of the perfusion experiment, again a biopsy was taken from the liver to determine the intracellular concentration of the substrate and perpetrator. The biopsies were snap frozen and immediately stored at ≤-70°C.

Table 3.1 - General properties on statins and rifampicin as perpetrator drug. mg oral doses applied *in vivo*, fraction absorbed and mg bolus applied to the portal vein of ex vivo perfused livers.

Substrate (victim drug)	Transporters involved	Metabolism	Fraction absorbed (%)	mg oral doses	mg bolus applied to *ex vivo* liver
Atorvastatin	NTCP, OATP1B1, OATP1B3 and OATP2B1[1,2]	CYP3A4[1,2]	12%[3]	10 mg[7]	0.104 mg
Pitavastatin	BCRP, NTCP, OATP1B1 and OATP1B3[1,2]	CYP2C9[3] CYP2C8	60%[3]	2 mg[3]	0.141 mg
Rosuvastatin	OATP1B1, OATP1B3, NTCP, MRP2, BCRP[1,2]	CYP2C9[4]	50%[5]	10 mg[8]	1.400 mg
Perpetrator drug					
Rifampicin			95%[6]	600 mg[1,2]	67.7 mg

[1] (2), [2] (1) , [3] (43), [4] (44) , [5](45) [6](46), [7](47), [8](29)

Bioanalysis

The concentration of atorvastatin and its metabolites, pitavastatin, rosuvastatin and rifampicin in plasma and bile were quantified using LC/MS. Briefly, 20 µL of sample was extracted by adding 100 µL of acetonitrile containing internal standard. Samples were vortexed, centrifuged at 3000 rpm for 5 minutes and 100 µL of supernatant was collected in a clean sample plate. Samples were then mixed with 50 µL of water, vortexed and injected into LC/MS for quantification. The details of LC/MS conditions used for the analysis of each compound are shown in Supplemental Table S3.2. The mass spectrometer (AB Sciex API 5500) was operated in electrospray positive ion mode with the capillary voltage of 5.5 kV and Spray temperature of 550°C. The multiple reaction monitoring transitions used for all the compounds are shown Supplemental Table S3.3.

Liver function assessment

During the perfusion experiment, blood gas analysis was executed every hour by measuring amongst others pH, pO_2, pCO_2, SO_2, glucose and lactate concentrations using a blood gas analyzer (iSTAT Alinity, Abbott). Additionally, hepatic artery and portal vein flow and resistance values were reported from the LiverAssist machine.

Multiple parameters were measured in perfusate and bile samples from the perfused livers to study liver viability. Total bilirubin, alanine transaminase (ALT) and aspartate transaminase (AST) concentration in the plasma and bile samples were measured using a Reflotron (Roche). Additionally, at the end of the perfusion period (360 min of perfusion) a bolus (10 mg) of Indocyanine green (ICG) was applied to the *ex vivo* liver to assess liver functionality by studying the clearance of ICG from the perfusate. Samples were taken at t=0, 1, 2, 4, 6, 8, 10, 15, 20, 30, 40, 50 and 60 min after dosing. Sample were centrifuged to obtain plasma and thereafter, 100 µl was sampled and measured at 788 emission and 813 excitation using a microplate reader (Tecan infinite m200 pro).

Liver perfusion studies were approved when the following acceptance criteria were met: 1) stable bile production and bile flow throughout the whole experiment, with >12 mL/h during 120 after 120 min of perfusion; 2) plasma bilirubin levels <20 µmol/L after 120 min of perfusion; 3) bile bilirubin levels >200 µmol/L after 120 min of perfusion; 4) plateau phase of AST and ALT reached within 60 min of perfusion; 5) plasma ICG reduced by 50% within 40 min after administration of ICG.

In total thirteen livers were perfused for a period of 420 min. Of these livers, three perfusions were excluded from the PK analysis to study DDI: one liver exposed to atorvastatin was excluded due to an experimental dosing error (Figure S3.1 and S3.2) and two livers exposed to pitavastatin showed acute hepatotoxic effects. The PK data of these livers is shown in the supplemental figures (Figure S3.1 and S3.2).

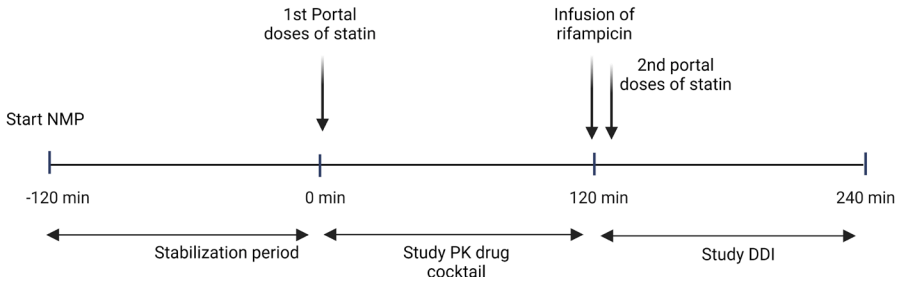

Figure 3.1 - Schematic representation of the experimental set-up. Livers were connected to the perfusion device and after 120 min a 10 min bolus (1mL/min) with a statin was administered to the liver. Plasma and bile samples were taken for 120 min. At t=120, rifampicin was administrated for 10 min at 1mL/min and at t=125 the second bolus of the statin was administrated. Subsequently plasma and bile samples were taken for the following 120 min.

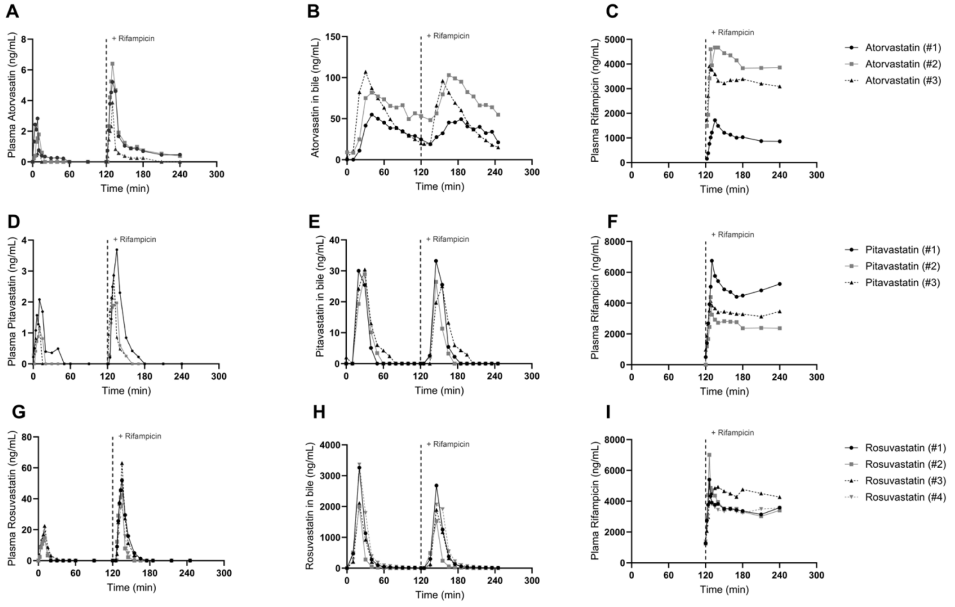

Figure 3.2 - Pharmacokinetic profile of atorvastatin (dosed as slow bolus of 0,104 mg over 10 min to portal vein) in plasma (A) and bile (B), pitavastatin (dosed as slow bolus of 0.141 mg over 10 min to portal vein) in plasma (D) and bile (E), and PK profile of rosuvastatin (dosed as slow bolus of 1.400 mg to portal vein) on plasma(G) and bile (H) Plasma pharmacokinetic profile of rifampicin (dosed as bolus of 67.7 mg to the portal vein) shown for each experiment (C,F and I)

Quantitative LC-MS/MS analysis of hepatic transporters in porcine and human livers

To study transporter and enzyme expression in porcine liver tissue compared to the expression in human liver tissue, from five healthy domestic pigs (*Sus scrofa domesticus*, 2 male and 3 female, age 10–14 weeks and body weight between 15 and 25 kg) was collected. These animals were additionally used for educational purposes at the Utrecht University (Utrecht, The Netherlands). The local animal welfare office approved the use of these animals for these purposes which was in full compliance with the aim to contribute to the reduction, refinement, and replacement of animal experiments. Before termination, pigs had free access to food and water. Liver tissue of domestic pigs was collected only when defined healthy as judged by a veterinarian.

Human liver samples derived from 15 individuals, of which 5 were anonymously collected at the University Medical center of Groningen (UMCG, Groningen, The Netherlands) and were kindly provided by Prof. Dr. G.M.M. Groothuis (University of Groningen, The Netherlands) and 10 were collected at the Department of Surgery, Uppsala University Hospital (Uppsala, Sweden) and were kindly provided by Prof. Dr. P. Artursson (7 male and 3 female donors; human liver specimens also used in previously published study[17]. Collection of redundant tissue from surgeries (collected as waste material) was approved by the Medical Ethical Committee of the UMCG or the Uppsala Ethical Review Board (ethical approval no. 2009/028 and 2011/037). No clinically relevant or identifiable information from the patients was collected.

To determine the protein levels of BCRP, BSEP, MDR1, MRP1, MRP2, OATP2B1, OCT1, GLUT1, MCT1, MRP3, NTCP, OATP1B1, OATP1B3 in porcine and human liver tissue, we followed the protocol of membrane isolation and trypsin digestion as previously described for tissue samples and cell lines ([18,19]). All samples were processed in duplicate. LC-MS/MS settings were as previously described (19). For each peptide 3 transitions were chosen (Q3–1, Q3–2, and Q3–3) for quantitation and confirmation (Supplemental Table S3.4). In case no suitable prototypic peptide could be selected for the human and porcine transporter proteins, two separate peptides were selected and synthesized (Supplemental Table S3.4). Peptides labeled with 15N and 13C (AQUA peptide) were synthesized (Sigma Aldrich Chemie, Steinheim, Germany) and used as an internal standard for quantification. For each peptide, a calibration curve of

0.01–50 ng/ml and quality controls were included in every run. Data are expressed as fmol transporter protein/mg liver.

Data analysis

Data obtained during the perfusion studies was analyzed using Graphpad prism version 8. Values for the area under the concentration time curve (AUC) were calculated using the linear trapezoidal method. The area under the concentration time curve ratio (AUCR) was determined by dividing the $AUC_{120\text{-}240\ min}$ / $AUC_{0\text{-}120\ min.}$ Student's *t* test was used to analyze differences between two groups.

Results

Assessment of liver functionality during perfusion

During the perfusion of the livers, flow and bile production were monitored. The perfused livers (n=3 for atorvastatin, n=3 for pitavastatin and n=4 for rosuvastatin) included in the PK analysis showing a stable portal and arterial flow of 1548±229 mL/min and 175±67 mL/min respectively and substantial bile production throughout the experiment (on average 79.2±27.6 mL in a period of 360 min) (Figure S3.1). With 57.1±15.7 mL, the livers exposed to pitavastatin produced the least amount of bile during the total perfusion period. For atorvastatin and rosuvastatin exposed livers, bile production was 78.9±24.7 mL and 107.2±12.5 mL respectively.

Plasma concentration profiles and biliary excretion of atorvastatin, pitavastatin and rosuvastatin

In order to study plasma and biliary clearance of the statins, atorvastatin (0.104 mg), pitavastatin (0.141 mg) or rosuvastatin (1.400 mg) was administered via the portal vein in a slow bolus (10 min, 1 mL/min), resulting in initial portal concentrations of 7.02 ng/mL, 8.50 ng/mL and 108.73 ng/mL for atorvastatin, pitavastatin and rosuvastatin respectively. During the dosing period and thereafter, multiple perfusate and bile samples were taken to assess the pharmacokinetic profile of the drugs. Sampling at the portal vein during the 10 min dosing period and simultaneously at the arterial side, enabled us to calculate the hepatic extraction ratio. Table 3.2 and Figure 3.2 show the plasma and biliary profile of the statins and plasma rifampicin concentration. The livers

showed a hepatic extraction ratio of 0.8±0.1 for all statins (Figure 3.2A-B, D-E, G-H, Table 3.2). Within 10 minutes after the start of the bolus administration, atorvastatin was detected in the bile with a T_{max} of 35.0±5.0 min. A total of 13.0±5.6% of the parent compound was secreted into the bile within 120 min of perfusion. Pitavastatin secretion into the bile was slower, and was detected in the bile 20 min after the start of the administration with a substantially lower total biliary excretion of 1.1±0.1% within 120 min. Rosuvastatin was detected in the bile 10 min after the start of the administration, reaching peak levels at 22.5±4.3 min. In total 10.1±2.5% rosuvastatin was excreted into the bile during 120 min of perfusion.

Table 3.2 – Overview of PK of atorvastatin, pitavastatin and rosuvastatin and the effect of rifampicin on the hepatic uptake and biliary clearance of these statins. Values are mean ± SD (n=3 for atorvastatin, n=3 for pitavastatin and n=4 for rosuvastatin).

Statin PK		Plasma			Bile		
		Substrate alone	*+ Rifampicin*	*Fold change*	*Substrate alone*	*+ Rifampicin*	*Fold change*
Atorvastatin	C_{max} (ng/mL)	1.79 ± 0.84	5.16 ± 1.03	2.88	216.88 ± 114.98	161.73 ± 86.17	0.75
	$AUC_{0-120\ min/\ 120-240\ min}$ (ng/mL)	18.09 ± 10.73	112.79 ± 46.06	7.24	13517.33 ± 5809.52	7780.25 ± 3676.67	0.58
	% biliary excretion	-	-	-	13.00 ± 5.59	7.48 ± 3.54	0.58
	Biliary clearance (L/h)	-	-	-	87.78 ± 78.42	6.31 ± 6.38	0.07
	Hepatic extraction ratio	0.82 ± 0.08	0.51 ± 0.09	0.62	-	-	-
Pitavastatin	C_{max} (ng/mL)	1.47 ± 0.43	2.43 ± 0.70	3.03	65.07 ± 7.27	72.12 ± 20.35	1.11
	$AUC_{0-120\ min/\ 120-240\ min}$ (ng/mL)	19.51 ± 11.89	32.64 ± 17.62	2.63	1448.33 ± 129.39	1288.33 ± 281.69	0.89
	% biliary excretion	-	-	-	1.03 ± 0.09	0.91 ± 0.20	0.89
	Biliary clearance (L/h)	-	-	-	5.33 ± 2.73	1.16 ± 0.86	0.22
	Hepatic extraction ratio	0.84 ± 0.01	0.72 ± 0.08	0.87	-	-	-
Rosuvastatin	C_{max} (ng/mL)	18.43 ± 3.15	48.28 ± 10.25	2.62	8927 ± 1302	6384.25 ± 207.58	0.72
	$AUC_{0-120\ min/\ 120-240\ min}$ (ng/mL)	186.57 ± 44.90	578.73 ± 152.91	3.10	140123 ± 34948	118572.00 ± 28916.47	0.85
	% biliary excretion	-	-	-	10.01 ± 2.50	8.47 ± 2.07	0.85
	Biliary clearance (L/h)	-	-	-	46.66 ± 13.27	13.18 ± 5.39	0.28
	Hepatic extraction ratio	0.82 ± 0.03	0.71 ± 0.07	0.87	-	-	-

Effect of rifampicin on statin kinetics and biliary clearance

To study the effect of rifampicin on statin plasma kinetics and biliary clearance, a second bolus of the statin was co-administrated with a bolus of rifampicin (67.7 mg). Upon co-administration of rifampicin, the plasma C_{max} increased ~3-fold for all statin drugs: from 1.8±0.8 ng/mL to 5.2±1.1 ng/mL for

atorvastatin, from 1.5±0.4 ng/mL to 4.5±1.9 ng/mL for pitavastatin and from 18.4±3.2 ng/mL to 48.3±10.3 ng/mL for rosuvastatin (Figure 3.2, Table 3.2). Additionally, all plasma AUCs of the statins increased upon co-administration of rifampicin: livers exposed to atorvastatin showed the highest AUC ratio (AUCR) of 7.2, followed by rosuvastatin (AUCR 3.1) and pitavastatin (AUCR 2.6) upon rifampicin co-administration (Figure 3.3A). In line with these data, the most profound effect of rifampicin on the hepatic extraction was also observed for atorvastatin that decreased from 0.8±0.1 to 0.5±0.1, while it decreased from 0.8±0.1 to 0.7±0.1 for both pitavastatin and rosuvastatin. The addition of rifampicin resulted in a biliary secretion of 6.80±3.85% of administered atorvastatin corresponding to 0.47-fold reduction in biliary clearance. Interestingly, a more profound reduction in biliary excretion was observed for rosuvastatin and pitavastatin upon co-administration with rifampicin, i.e., 0.15-fold and 0.11-fold, respectively.

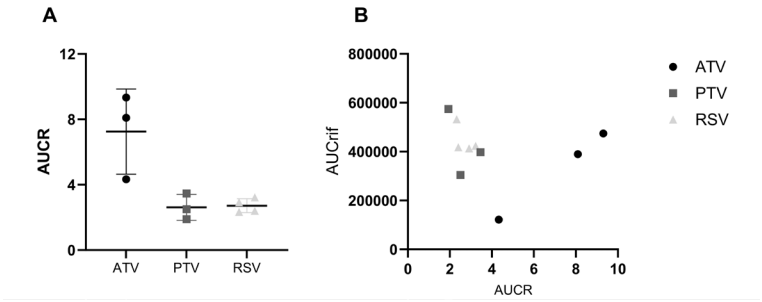

Figure 3.3 - (A) Showing the rank-order of DDI in AUCR for atorvastatin (ATV), pitavastatin (PTV) and rosuvastatin (RSV) (B) Relation of AUCR to $AUC_{rifampicin}$.

Pharmacokinetics of rifampicin

Figures 3.2C, F and I show the concentration time profile of the perpetrator rifampicin in the three statin groups. The livers exposed to atorvastatin showed the lowest C_{max}, 3.4± 1.3 µg/mL for rifampicin compared to livers exposed to pitavastatin (5.1± 1.2 µg/mL) and rosuvastatin (5.3±1.0 µg/mL; Figure 3.2C,F and I, Table 3.3). After administration, rifampicin was rapidly detected in the bile with a T_{max} of 46.7±4.7 min, 30.0±0.0 min and 35.0±11.2 min for livers exposed to atorvastatin, pitavastatin, and rosuvastatin respectively. The biliary clearance of rifampicin was 6.7±4.8%, 5.7±2.5%, 10.9±1.6% respectively in livers treated with atorvastatin, pitavastatin and rosuvastatin livers.

Table 3.3 - Overview of PK of rifampicin during ex vivo liver perfusion. Values are mean ± SD (n=3 for Atorvastatin, n=3 for pitavastatin and n=4 for rosuvastatin).

		Plasma	Bile
Atorvastatin	C_{max} (µg/mL)	3.43 ± 1.25	63.27 ± 31.08
	T_{max} (min)	15.33 ± 3.68	46.67 ± 4.71
	AUC $_{120\text{-}240min}$ (µg/mL)	328.58 ± 150.18	5622.59 ± 2934.09
	% biliary excretion	-	8.39 ± 4.38
Pitavastatin	C_{max} (µg/mL)	5.09 ± 1.18	64.96 ± 1.92
	T_{max} (min)	10.33 ± 2.05	30.00 ± 0.00
	AUC $_{120\text{-}240min}$ (µg/mL)	425.32 ± 111.98	4690.66 ± 1066.66
	% biliary excretion	-	7.00 ± 1.59
Rosuvastatin	C_{max} (µg/mL)	5.53 ± 0.95	88.18 ± 7.56
	T_{max} (min)	12.00 ± 1.00	35.00 ± 11.20
	AUC $_{120\text{-}240min}$ (µg/mL)	446.61 ± 49.48	7284.19 ± 1053.33
	% biliary excretion	-	10.87 ± 1.57

Metabolism of atorvastatin and the effect of rifampicin on metabolism

Since atorvastatin is subjected to CYP3A4 mediated hepatic metabolism, we also investigated the presence of its known metabolites (atorvastatin lactone, 2-OH atorvastatin, 2-OH atorvastatin lactone, 4-OH atorvastatin and 4-OH atorvastatin lactone) in plasma and bile samples obtained from the perfused livers exposed to atorvastatin (Figure 3.4, Table 3.3). All five clinically known metabolites were detected in the bile, but no metabolites were detected in plasma. For all metabolites, the biliary secretion was decreased upon the co-administration of rifampicin (Table 3.4). Main inhibition was shown for the metabolites atorvastatin lactone (AUCR of 0.1), followed by 2-OH atorvastatin (AUCR of 0.8) and 4-OH atorvastatin (AUCR of 0.7).

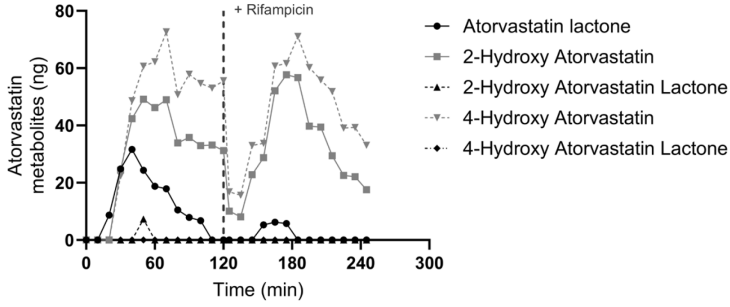

Figure 3.4 - Atorvastatin metabolite excretion into the bile (n=1) upon dosing atorvastatin (0,104 mg) to the portal vein of perfused porcine liver, before (0-120 min) and after co-administration with perpetrator rifampicin (125-245 min).

Table 3.4 - % Biliary excretion of atorvastatin (0.104 mg) metabolites for atorvastatin alone and atorvastatin + rifampicin n=1.

% biliary clearance of metabolites	Atorvastatin	Atorvastatin+ Rifampicin	AUCR
Atorvastatin lactone	1.45	0.17	0.11
2-hydroxy atorvastatin	3.49	2.64	0.76
2-hydroxy atorva lactone	0.07	0.00	0.00
4-hydroxy atorvastatin	4.91	3.33	0.68
4-hydroxy atorvastatin lactone	0.00	0.00	0.00

Bilirubin as potential endogenous biomarker for OATP function

Total bilirubin levels were measured in plasma and bile samples of the perfused livers (Figure 3.5), as bilirubin was recently recommended as an endogenous biomarker for OATP1B1/1B3 function[3,20]. Rifampicin, an inhibitor of multiple transporters including OATP1B1/1B3, should therefore also block the (re)uptake of (glucuronidated) bilirubin from the plasma. During the first 120 min of perfusion, when only the statins were administered to the livers, a stable concentration of plasma bilirubin was measured (Figure 3.5A). Upon rifampicin exposure (120-240 min of perfusion), an increase in total plasma bilirubin was measured in all livers. For all three statins, the $AUC_{120-240}/AUC_{0-120}$ ratio showed an mean ratio of 1.6 indicating interference of rifampicin on the hepatic uptake of (glucuronidated) bilirubin. Total bilirubin concentration in the bile decreased upon rifampicin exposure and a mean AUCR of 0.5±0.14 was measured (Figure 3.5B).

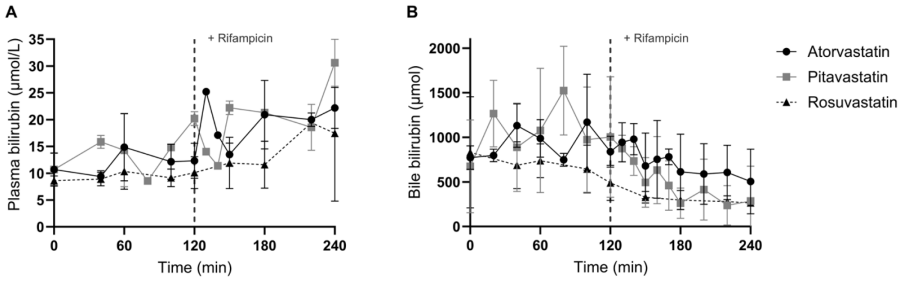

Figure 3.5 - Total bilirubin levels in plasma (A) en bile (B) of all liver perfusion experiments, discriminating atorvastatin (closed circles), pitavastatin (closed squares), and rosuvastatin (closed triangles), before (0-120 min) and after co-administration with perpetrator rifampicin (125-245 min).

First signs of drug induced toxicity by pitavastatin

Two out of 5 livers exposed to pitavastatin co-administrated with rifampicin were excluded from the PK analysis. Compared to the other three livers exposed to pitavastatin, these two livers demonstrated a delay in plasma clearance of pitavastatin and rifampicin with a plasma AUCR of 19.8 and 11.8 after the second bolus of pitavastatin (Figure 3.6A,C) and a lower hepatic extraction ratio of 0.5 for both affected livers (Figure 6H). Immediately after the second administration of pitavastatin, a reduction in the bile flow was observed for these two livers and the bile production completely stopped after 360 min of perfusion (Figure 3.6G). Upon the addition of rifampicin, these same livers showed an increase in plasma bilirubin compared to all the other perfused livers (60.1 µmol/L and 62.9 µmol/L at 360 min of perfusion) compared to the atorvastatin and rosuvastatin perfused livers (23.2±7.4 µmol/L at 360 min of perfusion) (Figure 6D). Plasma rifampicin concentrations were also elevated compared to the other livers exposed to pitavastatin (Figure 3.6C). To verify liver toxicity, plasma alanine aminotransferase (ALT) and aspartate transaminase (AST) levels were assessed (Figure 3.6E-F). The 2 livers showed increasing AST levels indicating induced liver toxicity. No effect on ALT was measured as all livers showed stable ALT levels reaching a plateau phase after 60 min (Figure 3.6F). Altogether, these results indicate a potential (start of) pitavastatin-induced hepatotoxicity in the form of impaired drug and bilirubin clearance and compromised bile production.

Protein expression of hepatic transporters

Figure 3.7 shows the absolute expression of drug transporters in liver tissue of porcine (domestic pig) and human origin. While the expression of the main transporter proteins BCRP, MDR1, MRP1, MRP2, GLUT1 and MCT1 was similarly abundant in porcine and human livers, the expression of OCT1 was approximately 1.8-fold higher in human livers compared to porcine livers ($P<0.001$). In contrast, the expression of BSEP, MRP3, NTCP, and OATP2B1 was 1.9, 1.7, 1.7 and 2.6 fold higher respectively in porcine livers than in human livers ($P<0.01$). OATP1B4 is the porcine ortholog for OATP1B1 and OATP1B3. The expression of OATP1B1 and OATP1B3 in human liver together, was significantly lower ($P<0.05$) to the protein expression level of OATP1B4 in porcine livers (2.8±1.0 fmol/mg tissue in human livers 5.8±1.8 fmol/mg tissue in porcine liver).

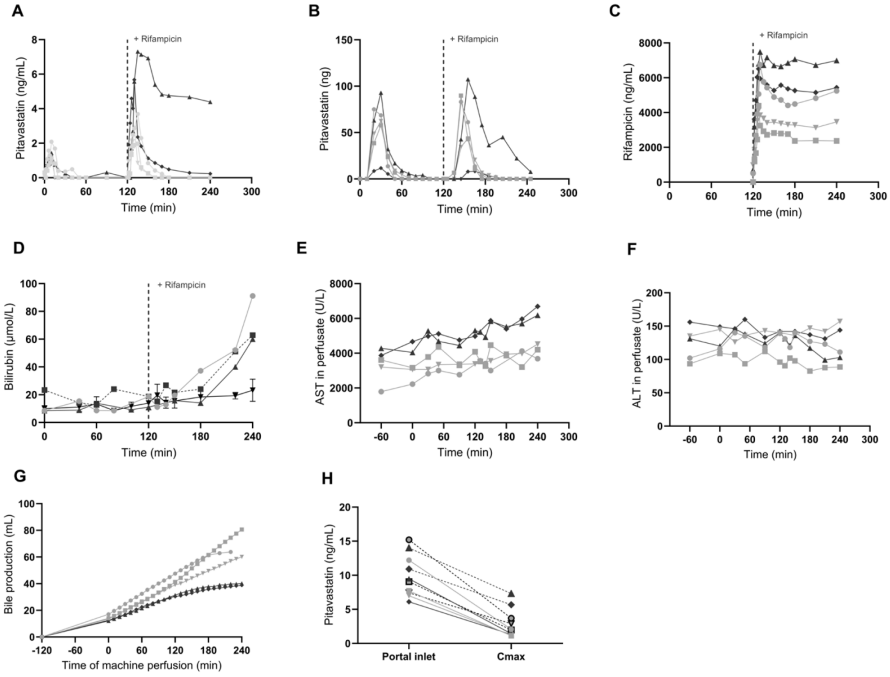

Figure 3.6 - First signs of drug induced liver toxicity in 2 of 5 livers exposed to pitavastatin (0.141 mg). These 2 livers are indicated with red lines, compared to the other three livers in grey. (A) plasma pitavastatin levels of 2 livers which showed signs of pitavastatin induced liver toxicity by the disability to take up pitavastatin compared to the other livers (B) biliary clearance of pitavastatin (C) plasma rifampicin concentration (D) plasma bilirubin increases dramatically after rifampicin co-administration compared to the atorvastatin and rosuvastatin perfused livers (black line) (E) plasma AST levels (F) plasma ALT levels and (G) total bile production during 360 min of perfusion (H) hepatic extraction during dosing *ex vivo* perfused livers (dotted lined represents the co-administration of rifampicin)

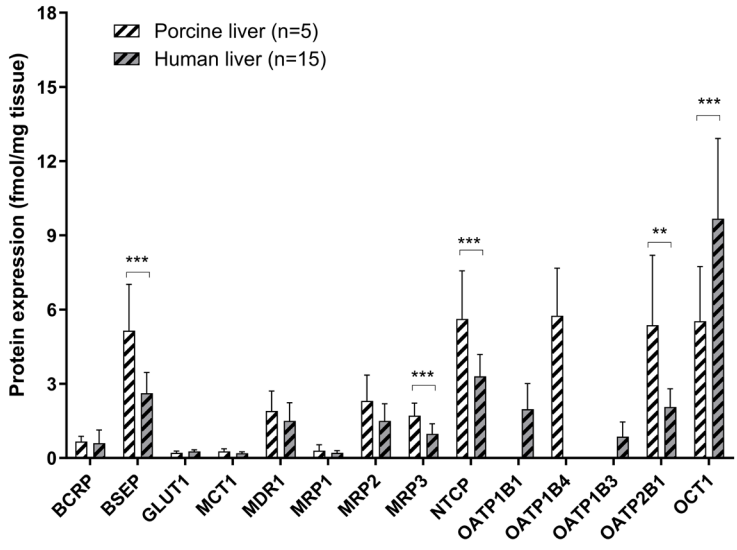

Figure 3.7 - Absolute expression (fmol/mg tissue) of various uptake and efflux transporter proteins within the plasma membrane of porcine livers (n=5) compared to the protein expression in human liver (n=15). Significant differences are denoted as asterisks (Students t-test * P<0.05, ** P<0.01, ***P<0.001).

Discussion

The ability to study biliary excretion and intracellular concentrations provides valuable information regarding metabolism and excretion of the drug. Thus far, to predict the hepatobiliary disposition of drugs, experimental studies have been performed using sandwich cultured hepatocytes, isolated perfused organ systems with rat livers or cannulated animal studies. In this study we perfused porcine livers using a novel advanced pressure driven perfusion machine, with a red blood cell-based perfusate which is suitable for normothermic and oxygenated conditions[12,21,22]. We describe for the first time the use of NMP of porcine livers to predict human hepatobiliary disposition – and DDI of drugs as demonstrated by using known OATP substrate drugs such as atorvastatin, pitavastatin and rosuvastatin with known OATP inhibitor, rifampicin as a perpetrator drug. Hepatobiliary toxicity in humans is poorly predicted from animal studies, primarily due to the fact that many animals differ markedly from humans in response to pharmacological agents[14]. In contrast to dogs, mice and rats, there is not much data on pigs in preclinical testing. Nevertheless, for

more complex research questions, *ex vivo* models from pig origin are regularly used to study intestinal absorption or the hepatic and biliary disposition of drugs[23-27]. In a comprehensive overview, Vaessen and co-workers provided protein and mRNA expression in human and pig intestinal tissues for a variety of transporters and enzymes. In general the protein and mRNA expression were well comparable between humans and pigs[19]. Furthermore, Elmorsi and co-workers recently showed a proteomic characterization of drug metabolizing enzymes and transporters in the pig liver showing the high resemblance with humans[15]. These data on transporters are in line with the proteomic data we show here comparing transporter protein expression in pig livers to the expression in human liver tissue. Except for the expression of BSEP, MRP3, NTCP, OATP2B1 and OCT1, no significant differences were observed in the expression of other transporter proteins. There is no porcine homologue for the human OATP1B1 however, porcine livers shown to express OATP1B4, which is the homologue of OATP1B3 showing 84% similarity ([15,28]).Although an almost 2-fold difference in human OATP1B1/1B3 vs pig OATP1B4 protein expression was observed, the obtained AUCR's were comparable to the human in vivo condition. Despite these differences, we here provide evidence that AUCR can be predicted by making use of ex vivo porcine NMP. The compounds tested are very good OATP (and NTCP) substrates and the results suggest that the hepatic uptake contributes to a similar percentage to the total clearance in humans and pigs. Other factors such as permeability differences between species and Km differences (for OATP-mediated uptake transporters) may compensate for the protein expression differences.

For this study, three statins were selected to study transporter-mediated DDI at the hepatic level. These statins, atorvastatin, rosuvastatin and pitavastatin, are listed as clinical substrates for the assessment of OATP1B1 and OATP1B3[2]. Additionally, the clearance of these drugs is mediated via diverse mechanism: CYP3A4 and OATP for atorvastatin, MRP2 and BCRP for rosuvastatin and BCRP for pitavastatin. All three statins showed to be good substrates for the uptake transporters, since a hepatic extraction ratio of >0.7 was observed. This is in line with clinically observed data[29,30] demonstrating that the experimental set-up is sufficient to predict the hepatic extraction ratio in humans.

In previous studies, statins have been applied to several preclinical models to predict rifampicin induced DDI. Bergman et al. performed an *in vivo* human study where rosuvastatin was administered into the jejunum via a Loc-I-Gut-

catheter[29]. The biliary clearance of rosuvastatin was measured after intestinal administration[29]. The C_{max} of rosuvastatin was detected 40 min after administration with a total biliary secretion of 11%; these data correspond very well to that from our experiments, showing a biliary secretion of 10%. Using the IPRL model, Lau et al. studied the interplay between transporters and enzymes in the disposition of atorvastatin (Lau et al. 2005). Compared to our porcine perfusion model, the IPRL model showed an extensively reduced interaction between atorvastatin and rifampicin. The biliary secretion in the IPRL model of atorvastatin was 7.4% while in our model the biliary clearance was 13.0±5.6%. Also, the effect of rifampicin on the inhibition of the biliary clearance was remarkably lower (21% in the IPRL vs. 50% in our model). The IPRL may therefore underpredict the DDI for atorvastatin and rifampicin. Together, these data show the IPRL model underpredicts the biliary clearance whereas a good comparability is observed between the porcine and human *in vivo* situation to the *ex vivo* perfused pig liver model. The metabolic activity of porcine livers during perfusion was shown by the presence of five different atorvastatin metabolites in the bile. The presence of all these metabolites in our study indicates that CYP3A4, CYP2C8 and UGT1A3 are metabolically active in the perfused pig liver[31-33].

In the experiments with atorvastatin, variability in AUCR was observed between replicates. Although rifampicin was administered in a similar slow bolus in each experiment, variability in plasma rifampicin concentrations were observed, possibly due to experimental handling and difference in total perfusate volume. Additionally, in clinical studies, the highest variation in AUCR is also observed for atorvastatin compared to the pitavastatin and rosuvastatin groups[1,2,34]. Our results showed a relation between plasma rifampicin AUC and AUCR for atorvastatin, while minor variation was observed for the pitavastatin and rosuvastatin group (Figure 3.3B). A comparable concentration-dependent inhibition effect of rifampicin on atorvastatin clearance was previously shown *in vivo* by Takehara et al. 2018 and Mori et al. 2019 and in vitro by Lau et al.[35]. Upon co-administration with rifampicin, the most profound effect was observed for atorvastatin (AUCR of 7.24), followed by rosuvastatin (AUCR of 3.07) and pitavastatin (AUCR of 3.03). As can be observed in Table 3.5, this same absolute AUCR as well as rank order of DDI magnitude was observed in studies with healthy volunteers[1,2,34].

Table 3.5 - Comparison of plasma AUCR between the NMP porcine liver model and in vivo studies. In all three clinical studies, the statins were dosed as a cocktail in healthy volunteers.

	NMP porcine liver model (current study)	Mori et al. 2019[1]	Takehara et al. 2018[2]	Prueksaritanont et al. 2016[34]
Atorvastatin	7.24	7.29	6.1	10.01
Pitavastatin	2.63	4.01	2.8	4.45
Rosuvastatin	3.10	2.48	2.4	5.38

In this study, pitavastatin exposure showed to affect hepatic function in 2 out of 5 perfused livers. Pitavastatin is one of the least prescribed statins[36] and although there are infrequent cases known of pitavastatin induced liver injury, it is known that pitavastatin can increase plasma AST, ALT and bilirubin concentration in the clinic[37-40]. Here, increased plasma AST was observed in 2 out of 5 livers exposed to pitavastatin. These same livers also showed the lowest bile production, the lowest bile bilirubin AUCR, the most profound effect on the hepatic extraction ratio and a prolonged ICG half-life (Figure S3.3). Together, these results indicate the first signs of acute drug-induced hepatoxicity. The therapeutic dose of pitavastatin is between 1–4 mg daily. However, the FDA prescribes not to exceed 2 mg once daily when patients also take rifampicin. Rifampicin significantly increases the Cmax of pitavastatin and therefore also increases the risk of rhabdomyolysis and myopathy[41]. In our study, the repeated dosing of pitavastatin could have resulted in hepatic injury due to affecting the ATP levels of the liver. Viola et al. showed a dramatic depletion of ATP in keratinocyte-irradiated cells which were exposed to pitavastatin[42]. Since the uptake and excretion of pitavastatin, bilirubin and rifampicin are ATP dependent processes, depletion of ATP resulted in a deteriorated functioning of these processes. A decrease in ATP levels may result in apoptosis and eventually necrosis[42]. This might be an explanation of our observations. To our knowledge, there is no other preclinical model which showed these acute adverse effects of pitavastatin in the liver.

Lately, the interest in endogenous biomarkers reflecting transporter involvement has increased. An example of such an endogenous biomarker is bilirubin. Due to the role of OATP1B1 and OATP1B3 in bilirubin uptake, bilirubin could serve as an endogenous biomarker for OATP1B1 and -1B3 related DDIs in the liver[3,20]. In our model, after administration of rifampicin, a direct increase in plasma bilirubin concentration was measured (AUCR 1.89) showing the direct inhibition of OATP-mediated hepatic uptake of (glucuronidated) bilirubin.

Furthermore, a decrease in biliary total bilirubin concentration was measured after the addition of rifampicin reflecting the inhibition of MRP2 and possibly UGT1A1. Unfortunately, no good correlation between plasma rifampicin concentration and plasma and bile bilirubin AUCR was observed, indicating that bilirubin fits more as a control marker rather than a precise biomarker. The current practice involves the use of CP-I, CP-III and conjugated bile salts as clinical biomarkers for OATP's[1]. Therefore, studies should incorporate these suggested biomarkers upon assessing DDI potential of drugs.

Conclusion

In conclusion, we have demonstrated that NMP of porcine livers is a potential novel and reliable model to study OATP-mediated DDI and its effect on hepatic clearance, biliary excretion and plasma (metabolite) profile of statins. Overall, the rank order of DDI severity indicated in our experiments is in good agreement with clinical data, the lowest DDI for pitavastatin and the highest for atorvastatin, indicating the potential importance of this new *ex vivo* model in early drug discovery.

Acknowledgement

We thank Angelique Speulman-Saat, Lisanne Pieters, Amber Zeeman and Mariska Gröllers-Mulderij for their excellent work in the lab and OrganAssist for their assistance. We thank Martin Paton of Takeda pharmaceutical Co. for his assistance with the bioanalytical assays.

References

1. Mori D, Kashihara Y, Yoshikado T, Kimura M, Hirota T, Matsuki S, Maeda K, et al. Effect of OATP1B1 genotypes on plasma concentrations of endogenous OATP1B1 substrates and drugs, and their association in healthy volunteers. Drug metabolism and pharmacokinetics 2019;34:78-86.
2. Takehara I, Yoshikado T, Ishigame K, Mori D, Furihata K-i, Watanabe N, Ando O, et al. Comparative study of the dose-dependence of OATP1B inhibition by rifampicin using probe drugs and endogenous substrates in healthy volunteers. Pharmaceutical research 2018;35: 1-13.
3. Chu X, Chan GH, Evers R. Identification of endogenous biomarkers to predict the propensity of drug candidates to cause hepatic or renal transporter-mediated drug-drug interactions. Journal of pharmaceutical sciences 2017;106:2357-2367.
4. Yang X, Gandhi YA, Duignan DB, Morris ME. Prediction of biliary excretion in rats and humans using molecular weight and quantitative structure–pharmacokinetic relationships. The AAPS journal 2009;11:511-525.
5. Fagerholm U. Prediction of human pharmacokinetics—biliary and intestinal clearance and enterohepatic circulation. Journal of Pharmacy and Pharmacology 2008;60:535-542.
6. Ito K, Iwatsubo T, Kanamitsu S, Ueda K, Suzuki H, Sugiyama Y. Prediction of pharmacokinetic alterations caused by drug-drug interactions: metabolic interaction in the liver. Pharmacological reviews 1998;50:387-412.
7. FDA. In Vitro Drug Interaction Studies — Cytochrome P450 Enzyme- and Transporter-Mediated Drug Interactions Guidance for Industry. In; 2020.
8. Stevens LJ, Donkers JM, Dubbeld J, Vaes WH, Knibbe CA, Alwayn IP, van de Steeg E. Towards human ex vivo organ perfusion models to elucidate drug pharmacokinetics in health and disease. Drug metabolism reviews 2020;52:438-454.
9. Guillouzo A. Liver cell models in in vitro toxicology. Environmental health perspectives 1998;106:511-532.
10. Chu X, Bleasby K, Evers R. Species differences in drug transporters and implications for translating preclinical findings to humans. Expert opinion on drug metabolism & toxicology 2013;9:237-252.
11. Gores GJ, Kost LJ, Larusso NF. The isolated perfused rat liver: conceptual and practical considerations. Hepatology 1986;6:511-517.
12. Borie DC, Eyraud D, Boleslawski E, Lemoine A, Sebagh M, Cramer DV, Roussi J, et al. FUNCTIONAL METABOLIC CHARACTERISTICS OF INTACT PIG LIVERS DURING PROLONGED EXTRACORPOREAL PERFUSION: POTENTIAL FOR A UNIQUE BIOLOGICAL LIVER-ASSIST DEVICE1. Transplantation 2001;72:393-405.
13. Eshmuminov D, Becker D, Borrego LB, Hefti M, Schuler MJ, Hagedorn C, Muller X, et al. An integrated perfusion machine preserves injured human livers for 1 week. Nature biotechnology 2020;38:189-198.
14. Helke KL, Swindle MM. Animal models of toxicology testing: the role of pigs. Expert opinion on drug metabolism & toxicology 2013;9:127-139.
15. Elmorsi Y, Al Feteisi H, Al-Majdoub ZM, Barber J, Rostami-Hodjegan A, Achour B. Proteomic characterisation of drug metabolising enzymes and drug transporters in pig liver. Xenobiotica 2020;50:1208-1219.
16. Varma MV, Obach RS, Rotter C, Miller HR, Chang G, Steyn SJ, El-Kattan A, et al. Physicochemical space for optimum oral bioavailability: contribution of human intestinal absorption and first-pass elimination. Journal of medicinal chemistry 2010;53:1098-1108.
17. Wegler C, Gaugaz FZ, Andersson TB, Wiśniewski JR, Busch D, Gröer C, Oswald S, et al. Variability in mass spectrometry-based quantification of clinically relevant drug transporters and drug metabolizing enzymes. Molecular pharmaceutics 2017;14:3142-3151.

18. Bosgra S, van de Steeg E, Vlaming ML, Verhoeckx KC, Huisman MT, Verwei M, Wortelboer HM. Predicting carrier-mediated hepatic disposition of rosuvastatin in man by scaling from individual transfected cell-lines in vitro using absolute transporter protein quantification and PBPK modeling. European Journal of Pharmaceutical Sciences 2014;65:156-166.
19. Vaessen SF, van Lipzig MM, Pieters RH, Krul CA, Wortelboer HM, van de Steeg E. Regional expression levels of drug transporters and metabolizing enzymes along the pig and human intestinal tract and comparison with Caco-2 cells. Drug Metabolism and Disposition 2017;45:353-360.
20. Fromm M. Prediction of Transporter-Mediated Drug–Drug Interactions Using Endogenous Compounds. Clinical Pharmacology & Therapeutics 2012;92:546-548.
21. Boehnert M, Yeung J, Bazerbachi F, Knaak J, Selzner N, McGilvray I, Rotstein O, et al. Normothermic acellular ex vivo liver perfusion reduces liver and bile duct injury of pig livers retrieved after cardiac death. American Journal of Transplantation 2013;13:1441-1449.
22. Watson CJ, Kosmoliaptsis V, Randle LV, Gimson AE, Brais R, Klinck JR, Hamed M, et al. Normothermic perfusion in the assessment and preservation of declined livers before transplantation: hyperoxia and vasoplegia—important lessons from the first 12 cases. Transplantation 2017;101:1084.
23. Anzenbacher P, Soucek P, Anzenbacherová E, Gut I, Hruby K, Svoboda Z, Kvetina J. Presence and activity of cytochrome P450 isoforms in minipig liver microsomes: comparison with human liver samples. Drug Metabolism and Disposition 1998;26:56-59.
24. Bergman E, Lundahl A, Fridblom P, Hedeland M, Bondesson U, Knutson L, Lennernäs H. Enterohepatic disposition of rosuvastatin in pigs and the impact of concomitant dosing with cyclosporine and gemfibrozil. Drug metabolism and disposition 2009;37:2349-2358.
25. Kararli TT. Comparison of the gastrointestinal anatomy, physiology, and biochemistry of humans and commonly used laboratory animals. Biopharmaceutics & drug disposition 1995;16:351-380.
26. Stevens LJ, van Lipzig MM, Erpelinck SL, Pronk A, van Gorp J, Wortelboer HM, van de Steeg E. A higher throughput and physiologically relevant two-compartmental human ex vivo intestinal tissue system for studying gastrointestinal processes. European Journal of Pharmaceutical Sciences 2019;137:104989.
27. Westerhout J, van de Steeg E, Grossouw D, Zeijdner EE, Krul CA, Verwei M, Wortelboer HM. A new approach to predict human intestinal absorption using porcine intestinal tissue and biorelevant matrices. European Journal of Pharmaceutical Sciences 2014;63:167-177.
28. Dalgaard L. Comparison of minipig, dog, monkey and human drug metabolism and disposition. Journal of pharmacological and toxicological methods 2015;74:80-92.
29. Bergman E, Forsell P, Tevell A, Persson EM, Hedeland M, Bondesson U, Knutson L, et al. Biliary secretion of rosuvastatin and bile acids in humans during the absorption phase. European journal of pharmaceutical sciences 2006;29:205-214.
30. Elsby R, Hilgendorf C, Fenner K. Understanding the critical disposition pathways of statins to assess drug–drug interaction risk during drug development: it's not just about OATP1B1. Clinical Pharmacology & Therapeutics 2012;92:584-598.
31. Lau Y, Huang Y, Frassetto L, Benet L. Effect of OATP1B transporter inhibition on the pharmacokinetics of atorvastatin in healthy volunteers. Clinical Pharmacology & Therapeutics 2007;81:194-204.
32. Riedmaier S, Klein K, Winter S, Hofmann U, Schwab M, Zanger UM. Paraoxonase (PON1 and PON3) polymorphisms: impact on liver expression and atorvastatin-lactone hydrolysis. Frontiers in Pharmacology 2011;2:41.
33. Lau YY, Okochi H, Huang Y, Benet LZ. Pharmacokinetics of atorvastatin and its hydroxy metabolites in rats and the effects of concomitant rifampicin single doses: relevance of first-pass effect from hepatic uptake transporters, and intestinal and hepatic metabolism. Drug metabolism and disposition 2006;34:1175-1181.
34. Prueksaritanont T, Tatosian D, Chu X, Railkar R, Evers R, Chavez-Eng C, Lutz R, et al. Validation of a microdose probe drug cocktail for clinical drug interaction assessments for drug transporters and CYP3A. Clinical Pharmacology & Therapeutics 2017;101:519-530.

35. Lau YY, Okochi H, Huang Y, Benet LZ. Multiple transporters affect the disposition of atorvastatin and its two active hydroxy metabolites: application of in vitro and ex situ systems. Journal of Pharmacology and Experimental Therapeutics 2006;316:762-771.
36. Amiri M. Worldwide statins prescription pattern: is it similar. Biom Biostat Int J 2020;9:194.
37. Kumar P, Mangla B, Singh S. Pitavastatin: A Potent Drug. Int J Pharma Res Health Sci 2018;6:2070-2074.
38. Teramoto T, Shimano H, Yokote K, Urashima M. New evidence on pitavastatin: efficacy and safety in clinical studies. Expert opinion on pharmacotherapy 2010;11:817-828.
39. Bhatti H, Tadi P. Pitavastatin. StatPearls [Internet] 2020.
40. Thapar M, Russo MW, Bonkovsky HL. Statins and liver injury. Gastroenterology & hepatology 2013;9:605.
41. FDA. LIVALO (pitavastatin) tablets, for oral use. In; 2009.
42. Viola G, Grobelny P, Linardi MA, Salvador A, Dall'Acqua S, Sobotta Ł, Mielcarek J, et al. Pitavastatin, a new HMG-CoA reductase inhibitor, induces phototoxicity in human keratinocytes NCTC-2544 through the formation of benzophenanthridine-like photoproducts. Archives of toxicology 2012;86:483-496.
43. Mukhtar R, Reid J, Reckless J. Pitavastatin. International journal of clinical practice 2005;59: 239-252.
44. Schneck DW, Birmingham BK, Zalikowski JA, Mitchell PD, Wang Y, Martin PD, Lasseter KC, et al. The effect of gemfibrozil on the pharmacokinetics of rosuvastatin. Clinical Pharmacology & Therapeutics 2004;75:455-463.
45. Sjöberg Å, Lutz M, Tannergren C, Wingolf C, Borde A, Ungell A-L. Comprehensive study on regional human intestinal permeability and prediction of fraction absorbed of drugs using the Ussing chamber technique. European Journal of Pharmaceutical Sciences 2013;48:166-180.
46. Zwolska Z, Niemirowska-Mikulska H, Augustynowicz-Kopec E, Walkiewicz R, Stambrowska H, Safianowska A, Grubek-Jaworska H. Bioavailability of rifampicin, isoniazid and pyrazinamide from fixed-dose combination capsules. The International Journal of Tuberculosis and Lung Disease 1998;2:824-830.
47. Lennernäs H. Clinical pharmacokinetics of atorvastatin. Clinical pharmacokinetics 2003;42:1141-1160.
48. Kamiie J, Ohtsuki S, Iwase R, Ohmine K, Katsukura Y, Yanai K, Sekine Y, et al. Quantitative atlas of membrane transporter proteins: development and application of a highly sensitive simultaneous LC/MS/MS method combined with novel in-silico peptide selection criteria. Pharmaceutical research 2008;25:1469-1483.

.

Supplementary materials

Table S3.1 - Perfusate composition.

Components	Quantity
Red blood cells	1000 mL
Plasma	1000 mL
Calcium gluconate (10%)	10 mL
Sodium bicarbonate 8.4% solution	To pH of 7.4
Heparin	1000 IU
Fast-acting insulin	Continuous infusion (10 U/mL; 1mL/h)
Taurocholate	Continuous infusion (2% w/v; 10 mL/h)
Epoprostenol	Continuous infusion (80 µg in 100 mL; 10mL/h)
Heparin	Continuous infusion 1041 U/h (1mL/h)
	Continuous infusion
Vitamin solution,	(1 mL/hr)
L-glutamine,	(1 mL/hr)
MEM essential acids and	(2 mL/hr)
Glutamax	(1 mL/hr)

Table S3.2 - Details of the LC/MS conditions used for the analysis of atorvastatin and atorvastatin metabolites, pitavastatin, rosuvastatin and rifampicin.

Compound	Column	Mobile Phase A	Mobile Phase B	Time (sec)	Mobile Phase B (%)	Flow (ml/min)
Atorvastatin, atorvastatin lactone, 2-hydroxy atorvastatin, 4-hydroxy-atorvastatin, 4-hydroxy atorvastatin lactone	Macmod; ACE 3 C18-AR; 30x2.1 mm	0.1% Formic Acid in 95:5 Water:Acetonitrile	0.1% Formic Acid in 50:50 Acetonitrile:Methanol	15 (Step) 60 (Ramp) 5 (Ramp) 30 (Step)	45 95 95 95	0.800
Pitavastatin				15 (Step) 60 (Ramp) 5 (Ramp) 30 (Step) 40 (Step)	30 70 95 95 30	
Rosuvastatin				15 (Step) 60 (Ramp) 30 (Step) 40 (Step)	40 80 95 40	
Rifampicin	Waters; Xbridge C8; 50x2.1 mm			30 (Step) 120(Ramp) 50 (Step) 40 (Step)	30 70 95 30	0.700

Table S3.3 - The Multiple Reaction Monitoring Transition (MRM) of Compounds.

Compound	MRM Transition(m/z)
Atorvastatin	559.30→466.00
Atorvastatin lactone	541.30→448.10
2-hydroxy atorvastatin	575.40→440.00
2-hydroxy atorvastatin lactone	557.30→448.10
4-hydroxy atorvastatin	575.30→440.20
4-hydroxy atorvastatin lactone	557.40→448.10
Pitavastatin	422.20→318.10
Rosuvastatin	482.10→258.20
Rifampicin	823.50→399.20
Glyburide (internal standard)	494.20→369.10
Carbamazepine (internal standard)	237.10→194.10
Rifampicin_d3 (internal standard)	826.50→794.70
Chrysin (internal standard)	255.10→153.00

Table S3.4 - Multiple reaction monitoring (MRM) transitions of the various peptides and the corresponding internal standard (AQUA) used. The peptide sequences were chosen according to the in silico peptide criteria defined by Kamiie et al.[48] and are exclusively present in the selected protein of interest.

Name	Labelled	Peptide sequence[a]	MW	Q1	Q3-1	Q3-2	Q3-3
BCRP	unlabelled	SSLLDVLAAR	1.044.2	522.8	644.3	757.5	529.4
	AQUA	SSLLDV**L**AAR	1.060.2	526.3	651.3		
BSEP	unlabelled	STALQLIQR	1.029.2	515.3	657.4	841.6	529.4
	AQUA	STALQ**L**IQR	1.045.2	518.8	664.3		
GLUT-1	unlabelled	VTILELFR	990.2	495.8	790.5	677.4	201.2
	AQUA	VTILELFR	1.00.2	500.8	800.5		
MCT-1	unlabelled	SITVFFK	841.0	421.2	173.3	641.3	201.1
	AQUA	SITVFFK	851.0	426.2	651.3		
MDR1	unlabelled	AGAVAEEVLAAIR	1269.5	467.7	719.4	216.1	618.4
	AQUA	AGAVAEEV**L**AAIR	1276.5	471.2	726.5		
MRP-1	unlabelled	TPSGNLVNR	957.1	479.2	428.8	759.4	672.4
	AQUA	TPSGNLVNR	973.1	482.7	432.3		
MRP2	unlabelled	VLGPNGLLK	910.1	455.8	698.5	185.3	213.3
	AQUA	VLGPNGL**L**K	926.1	459.2	705.4		
MRP3	unlabelled	ALVITNSVK	944.1	472.8	760.4	661.4	548.4
	AQUA	ALVITNS**V**K	950.1	475.8	766.5		
NTCP-pig	unlabelled	GIYDGTLK	866.0	433.7	696.3	143.2	171.2
	AQUA	GIYDGT**L**K	882.0	437.2	703.4		
NTCP-human	unlabelled	GIYDGDLK	880.0	440.7	710.3	143.2	171.2
	AQUA	GIYDGDLK	896.0	444.2	717.3		
OATP-1B1	unlabelled	LNTVGIAK	815.0	408.2	399.4	588.3	288.2
	AQUA	LNTVG**I**AK	831.0	411.7	402.9		
OATP-1B3	unlabelled	IYNSVFFGR	1.102.3	551.8	826.5	249.1	526.2
	AQUA	IYNSVF**F**GR	1.112.3	556.8	836.4		
OATP-1B4-pig	unlabelled	LTLVGIAK	816.0	408.2	399.4	588.3	288.2
	AQUA	LTLVG**I**AK	832.0	411.7	402.9		
OATP-2B1	unlabelled	SSISTVEK	849.9	425.7	563.3	676.3	175.1
	AQUA	SSIST**V**EK	855.9	428.7	569.3		
OCT-1	unlabelled	LPPADLK	752.9	377.2	543.3	183.3	260.3
	AQUA	LPPAD**L**K	768.9	380.7	550.4		

Table S3.5 - Absolute expression (fmol/mg tissue) of various uptake and efflux transporter proteins within the plasma membrane of porcine livers (n=5) compared to the protein expression in human liver (n=15). Values are mean ± SD. (ND = non detected).

	Porcine livers (n=5)	Human livers (n=15)
BCRP	0.66 ±0.20	0.60 ±0.52
BSEP	5.15 ±1.77	2.62 ±0.82
GLUT-1	0.20 ±0.08	0.27 ±0.06
MCT1	0.27 ±0.09	0.19 ±0.05
MDR1	1.90 ±0.76	1.50 ±0.71
MRP1	0.30 ±0.23	0.21 ±0.09
MRP2	2.31 ±0.99	1.50 ±0.68
MRP3	1.71 ±0.48	0.98 ± 0.39
NTCP	5.62 ±1.82	3.30 ±0.86
OATP1B1	ND	1.97 ±1.01
OATP1B4	5.76 ±1.79	ND
OATP1B3	ND	0.86 ±0.58
OATP2B1	5.37 ±2.68	2.06 ±0.71
OCT1	5.53 ± 2.09	9.68 ±3.16

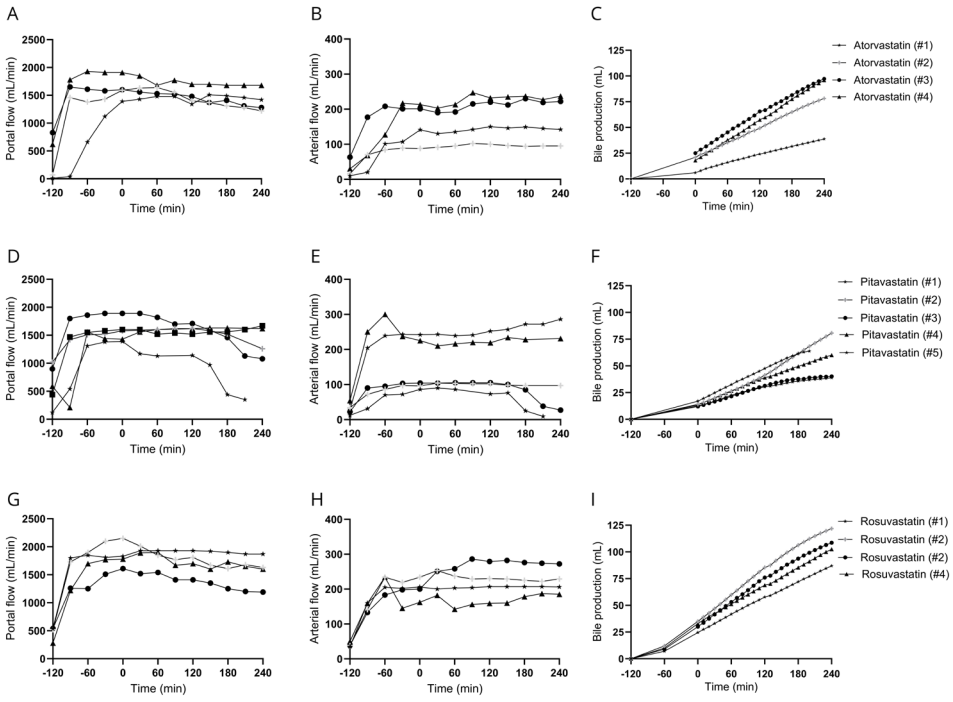

Figure S3.1 - Flow characteristics of all porcine livers during 360 min of normothermic perfusion, showing portal flow (A, D and G), arterial flow (B, E and H) and the cumulative bile production (C,F and I) livers exposed to atorvastatin, pitavastatin and rosuvastatin, respectively.

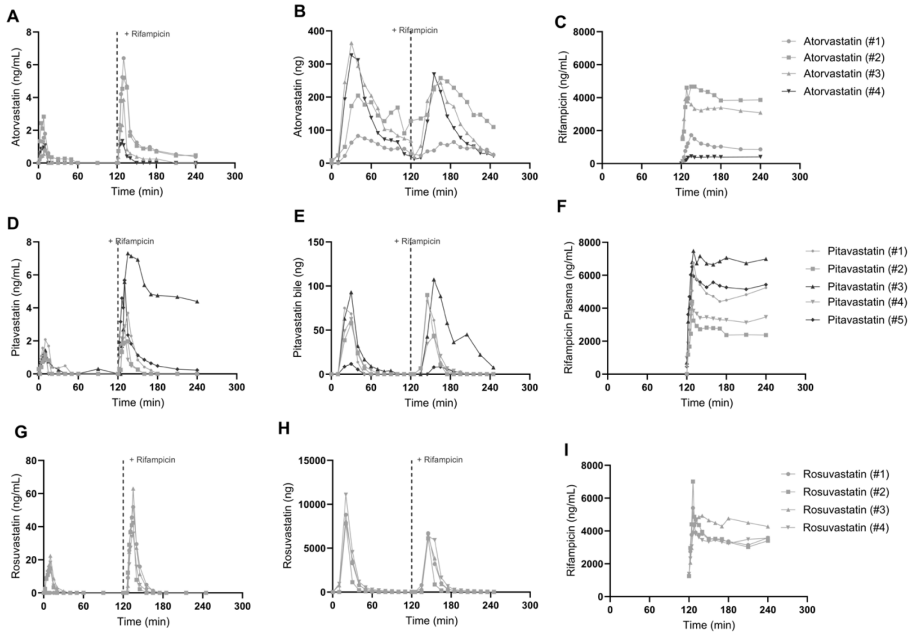

Figure S3.2 – Plasma en bile pharmacokinetic profiles of all perfused livers (n=14). Data excluded from PK analysis are represented with a black line, included data are presented in grey. PK of atorvastatin in (A) plasma and (B) bile, (C) showing the plasma rifampicin concentration of the livers exposed to atorvastatin, (D) PK of pitavastatin in plasma and (E) bile and (F) the plasma profile of rifampicin in livers exposed to pitavastatin. (G) PK of rosuvastatin in plasma and (H) bile and the plasma concentration of rifampicin in livers exposed to rosuvastatin

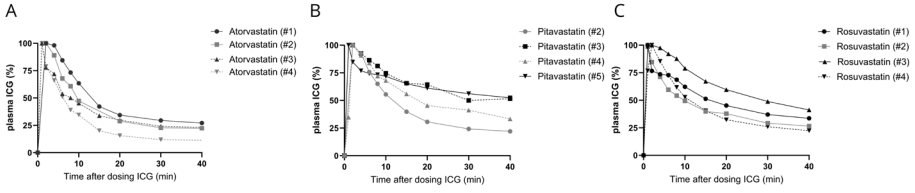

Figure S3.3 – indocyanine green (ICG) clearance from plasma upon dosing ICG as an IV bolus (10 mg) to the perfusate 360 min after starting the liver perfusion and exposing livers to atorvastatin 1-4 (A), pitavastatin 2-5 (pitavastatin 1 NA: due to decrease in portal and arterial and bile flow) (B) and rosuvastatin (C).


drug
cocktail